ICANS-VI

INTERNATIONAL COLLABORATION ON ADVANCED NEUTRON SOURCES

June 27 - July 2, 1982

THE IPNS TIME-OF-FLIGHT SINGLE CRYSTAL DIFFRACTOMETER

A. J. Schultz, R. G. Teller and Jack M. Williams

Chemistry Division, Argonne National Laboratory
Argonne, Illinois 60435, U.S.A.

The single crystal diffractometer (SCD) at the Argonne Intense Pulsed Neutron Source (IPNS) utilizes the time-of-flight (TOF) Laue technique to provide a three-dimensional sampling of reciprocal space during each pulse. The instrument contains a unique neutron position-sensitive ^{6}Li-glass scintillation detector with an active area of 30x30 cm. The three-dimensional nature of the data is very useful for fast, efficient measurement of Bragg intensities and for the studies of superlattice and diffuse scattering. The instrument was designed to achieve a resolution of 2% or better ($R = \Delta Q/Q$) with $2\theta > 60°$ and $\lambda > 0.7\text{Å}$.

THE IPNS TIME-OF-FLIGHT SINGLE CRYSTAL DIFFRACTOMETER

A. J. Schultz, R. G. Teller and Jack M. Williams
Chemistry Division
Argonne National Laboratory
Argonne, Illinois 60435

I. INTRODUCTION

The single crystal diffractometer (SCD)[1,2] at the Argonne Intense Pulsed Neutron Source (IPNS) is designed to provide fast, efficient data collection over a large solid angle and a large $|Q|$ range in reciprocal space. The major component of the instrument is a neutron position sensitive ^{6}Li-glass scintillation detector with an active area of 30 x 30 cm.[3]

As shown in Figure 1, the area detector and multiwavelength incident neutron radiation provide a three-dimensional sampling of reciprocal space during each pulse. In combination with a high

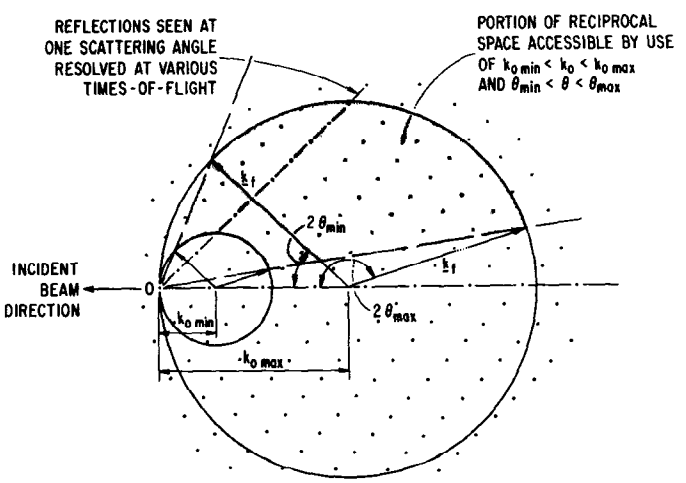

Fig. 1. Construction in reciprocal space to illustrate the use of multiwavelength radiation in single crystal diffraction. The circles with radii $k_{o\,max} = 1/\lambda_{min}$ and $k_{o\,min} = 1/\lambda_{max}$ are drawn through the origin. All reciprocal lattice points within the shaded area may be sampled by a large position-sensitive detector.

intensity pulsed source this can lead to higher data rates or the use of smaller crystals. The three-dimensional nature of the data can also be extremely useful in studying superlattice and scattering and diffuse scattering.

2. INSTRUMENT DESIGN[1,2]

The crystal and detector orienter incorporates all 4 circles which are normally found with conventional diffractometers (see Fig. 2). The detector is mounted on a 0.5 m. detector arm which permits sample-to-detector distances of 20 to 45 cm. and an accessible 2θ range of 20-160°. A Displex closed cycle helium refrigerator can be mounted on the diffractometer to permit sample temperatures in the range of 10-300 K. The sample is 663 cm. from the moderator surface, of which it "sees" a circular portion 8.8 cm in diameter. A low efficiency BF_3 counter is 30 cm. upstream from the sample and is used to monitor the incident neutron flux.

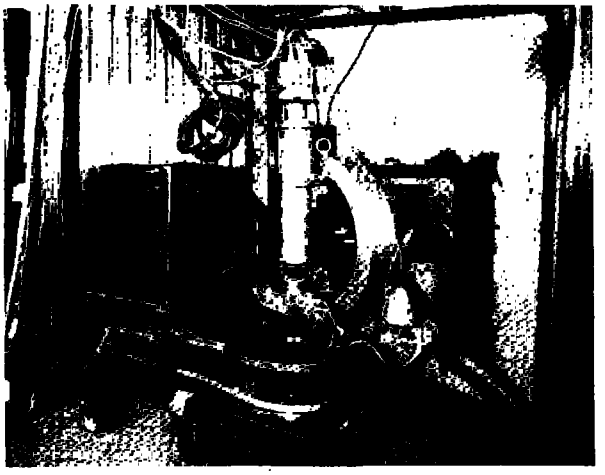

Fig. 2. Photograph of the Single Crystal diffractometer. The area detector is inside the shielded enclosure on the detector arm. A Displex helium refrigerator mounted on the goniostat permits sample temperatures of 10-300 K.

3. DETECTOR DESCRIPTION[3,4]

Over the past few years a program to develop a neutron position-sensitive detector, based on the Anger γ-ray camera principle, has been carried out at Argonne. The new detector has a number of important advantages relative to the conventional ^{3}He gas-filled multiwire proportional counter, as listed in Table I. Most important is higher efficiency at shorter wavelengths where the density of Bragg reflections is highest (Fig.3).

TABLE I. Inherent advantages of Scintillation Detector Vs. Proportional Counter

HIGHER DETECTION EFFICIENCY:	Particularly above 0.025 eV (Below 1.8 Å)
HIGHER COUNT-RATE CAPABILITIES:	No slow positive-ion collection
THINNER DETECTION MEDIUM:	Virtually parrallax free
THINNER WINDOW:	Virtually windowless
MORE FLEXIBLE CONFIGURATION:	No inherent shape or size limitations
MORE RUGGED:	No fragile anode, no microphonics, no gas leakage or contamination
GREATER CONSTRUCTION SIMPLICITY:	Requires no special fabrication facilities

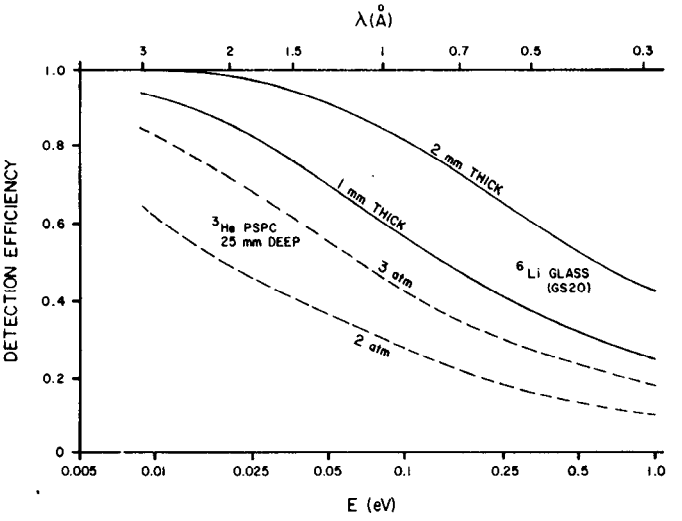

Fig. 3 Plots of neutron detector efficiency vs. wavelength for ^{3}He gas and ^{6}Li glass.

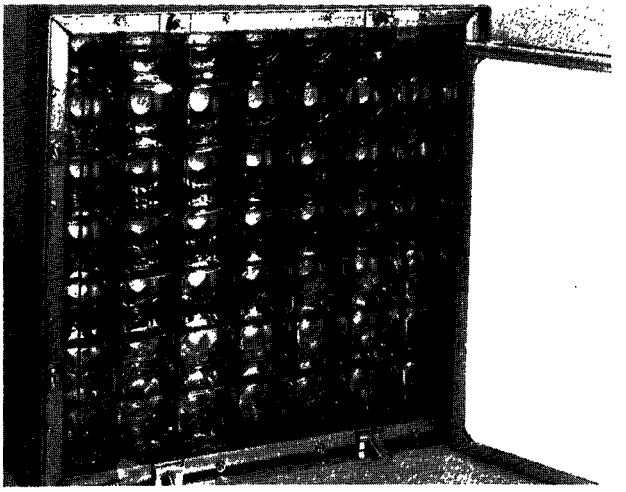

Fig. 4. Neutron-position scintillation detector consisting of a 7x7 array of square photomultiplier tubes, each 51x51 mm^2 and a 30x30 cm^2 ^{6}Li glass scintillator shown at the lower right removed from in front of the light disperser.

A photograph of the detector now in use on the SCD is shown in Figure 4, and a schematic drawing is shown in Figure 5. The detector contains a 2 mm. thick ^{6}Li-loaded, Ce-activated, glass scintillator, a 38 mm. thick light disperser consisting of Pyrex glass and plexiglass, and a 7x7 array of 2-inch square photomultiplier tubes (PMT's). A small air gap (0.1 mm.) between the scintillator glass and the light disperser provides a critical refraction angle of 40° which spreads the light over at least two PMT's in the horizontal and vertical directions. Incident light rays with angles greater than 40° are reflected and then scattered back by the layer of aluminum oxide on the opposite side of the scintillator.

The signal from each PMT is resistively weighted according to X and Y positions, respectively. The weighted sums for X and Y are divided by the unweighted sum to provide the centroid of the scintillation event. We estimate the intrinsic resolution of the detector is approximately 3.5 mm.

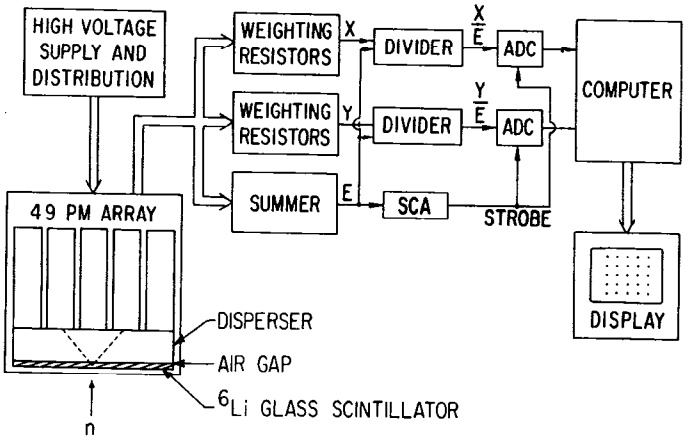

Fig. 5. Basic operation of neutron-position scintillation detector. The position of a neutron interaction in the ^{6}Li glass is determined by calculating the normalized centroids of scintillation X/E and Y/E using a resistor weighting scheme.

4. DATA ACQUISITION SYSTEM[5]

The data acquisition system (DAS) for the SCD consists of a PDP 11/34 computer with both a CRT and a printer terminal for user interaction, two 10-Mbyte RL02 disk drives, a magnetic tape drive, a color CRT graphics display terminal, and an interface to a CAMAC crate containing the motor controller for the goniostat. The PDP 11/34 is also interfaced to a multibus which links to a Z8001 microcomputer, 2.5 Mbytes of random access memory, and a second CAMAC crate used for data acquisi tion which contains a first-in-first-out (FIFO) buffer memory and the TOF clock. The digitized X and Y positions from the detector ADC are initially stored in the FIFO memory along with the digitized TOF. The Z8001 microcomputer histograms data from the FIFO memory in the random access memory using a user-generated look-up table. A typical histogram may have dimensions of 85x85x120, corresponding to X and Y on the detector and TOF, respectively (Fig. 6).

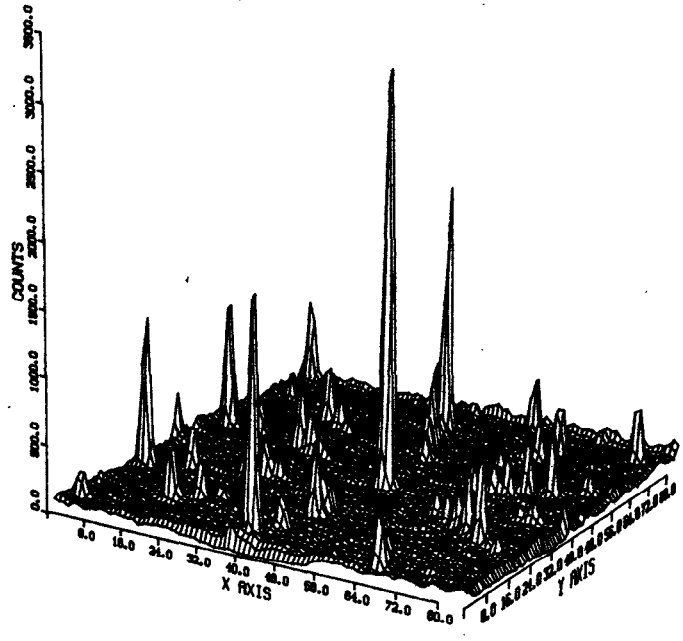

Fig. 6. A portion of a Laue pattern. The X and Y axes represent X and Y channel numbers corresponding to positions on the detector face. The counts for each X,Y bin have been summed over a wavelength range of 1-3 Å. Since there are 117 time, or wavelength channels, all of the Bragg peaks are easily resolved in the 3-D histogram.

5. DEADTIME LOSS

In addition to the three-dimensional histogram, a TOF spectrum is obtained from a low efficiency BF_3 proportional counter in the direct beam between the source and the crystal. As shown in Figure 7, whenever an event is obtained from the BF_3 monitor detector, the area detector is sampled to see if it is busy processing an event. If the 2-D detector is busy, the proper time channel of the deadtime loss histogram is incremented. The fractional deadtime loss for each time channel is then the number of lost events N_L divided by the number of monitor events N_T.

Since data rates may vary by a factor of 50 during each pulse, the data must be corrected for deadtime based on its TOF. Our experience at this time is that for a wavelength range of 0.7 to 3.5 Å (TOF = 1.2 to 6.1 msec.), depending on the sample, the percent deadtime loss may range from a maximum of 10-20% at the short wavelength end of the spectrum to 0% at the longest

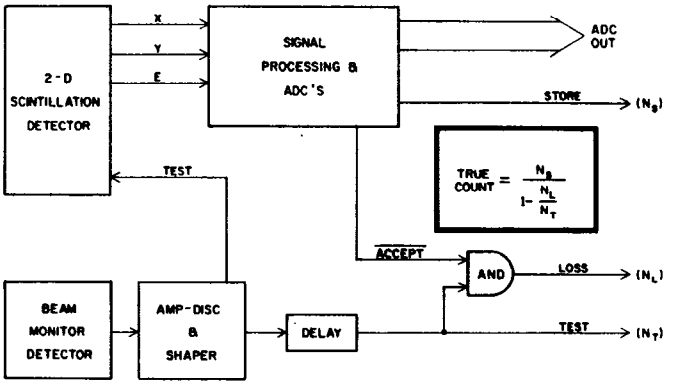

Fig. 7. Deadtime correction scheme. An event in the BF_3 beam monitor detector triggers a test pulse to the 2-D detector. If the test pulse is not accepted a deadtime loss event is added to the appropriate TOF histogram channel.

wavelength. From observed counting rates, we estimate this represents an average deadtime of approximately 7 μsec. This number includes the rejection of signals which do not fall within the pulse-height discriminator window (e. g., gamma-rays) or have been effected by pileup. Since the pulse risetime of the ^{6}Li glass is 0.5 μsec. (90% of final amplitude), improvements in shielding, background levels, signal shaping and position encoding could lead to a smaller deadtime.

6. RESOLUTION

The resolution function of the instrument is

$$R_S = \frac{\Delta S}{S} = [R_t^2 + R_L^2 + (\cot\theta \cdot \Delta\theta)^2]^{\frac{1}{2}}$$

where $S = \frac{2\sin\theta}{\lambda} = (2m/h)(L/t)\sin\theta$ and t is the time-of-flight, L is the neutron flight distance, θ is the Bragg angle, λ is the neutron wavelength, m is the neutron mass, and h is Planck's constant. Reasonable values for the variables in the resolution function are $R_t = 0.017$, $R_L = 0.0015$ and $\Delta\theta = 0.85°$. By varying the time channel width such that Δt/t is constant, these values are wavelength independent and R_S is 2θ dependent due to the cotθ function. However, above $2\theta = 60°$ the contribution to R_S becomes small, and R_S quickly approaches or falls below a value of 0.02. To resolve a 25 Å axis at the d-spacing of 1 Å only requires 4% resolution, such that the SCD resolution is sufficient for single crystal studies of mose molecular compounds with upwards of 100 independent atoms in the unit cell.

REFERENCES

[1]S. W. Peterson, A. H. Reis, Jr., A. J. Schultz and P. Day, Advances in Chemistry Series, No. 186, Solid State Chemistry: A Contemporary Overview, S. L. Holt, J. B. Milstern and M. Robbins, eds., American Chemical Society, 1970, pp. 75-91.

[2]A. J. Schultz, R. G. Teller, J. M. Williams, M. G. Strauss and R. Brenner, Trans, Am. Cryst. Assoc., Vol. 18, 1982, in press.

[3]A. J. Schultz, R. G. Teller, S. W. Peterson and J. M. Williams, Transactions of the Symposium on Neutron Scattering, Argonne National Laboratory, August 12-14, 1981, American Institute of Physics, J. Faber, ed., in press.

[4]M. G. Strauss, R. Brenner, F. J. Lynch and C. B. Morgan, IEEE Trans. Nucl. Sci., NS-28, 800 (1981).

[5]R. K. Crawford, R. T. Daly, J. R. Baumann, C. B. Morgan, G. E. Ostrowski and T. G. Worlton, IEEE Trans. Nucl. Sci., NS-28, 3692 (1981).